

# High latitude Galactic dust emission in the BOOMERanG maps

S. Masi<sup>1</sup>, P.A.R. Ade<sup>2</sup>, J.J. Bock<sup>3,4</sup>, A. Boscaleri<sup>5</sup>, B.P. Crill<sup>3</sup>, P. de Bernardis<sup>1</sup>, M. Giacometti<sup>1</sup>, E. Hivon<sup>3</sup>, V.V. Hristov<sup>3</sup>, A.E. Lange<sup>3</sup>, P.D. Mauskopf<sup>6</sup>, T. Montroy<sup>7</sup>, C.B. Netterfield<sup>8</sup>, E. Pascale<sup>5</sup>, F. Piacentini<sup>1</sup>, S. Prunet<sup>8</sup>, J. Ruhl<sup>7</sup>

<sup>1</sup> Dipartimento di Fisica, Universita' La Sapienza, Roma, Italy

<sup>2</sup> QMWC London UK

<sup>3</sup> CALTECH, Pasadena, USA

<sup>4</sup> JPL, Pasadena, USA

<sup>5</sup> IROE-CNR, Firenze, Italy

<sup>6</sup> Department of Astronomy, Univ. of Wales, UK

<sup>7</sup> Department of Astronomy, Univ. of California at Santa Barbara, USA

<sup>8</sup> Department of Astronomy, Univ. of Toronto, Canada

Received \_\_\_\_\_; accepted \_\_\_\_\_

submitted to The Astrophysical Journal, 30/jan/2000

## ABSTRACT

We present mm-wave observations obtained by the BOOMERanG experiment of Galactic emission at intermediate and high ( $b < -20^\circ$ ) Galactic latitudes. We find that this emission is well correlated with extrapolation of the IRAS-DIRBE maps, and is spectrally consistent with thermal emission from interstellar dust (ISD). The ISD brightness in the 410 GHz map has an angular power spectrum  $c_\ell \sim \ell^{-\beta}$  with  $2 \lesssim \beta \lesssim 3$ . At 150 GHz and at multipoles  $\ell \sim 200$  the angular power spectrum of the IRAS-correlated dust signal is estimated to be  $\ell(\ell+1)c_\ell/2\pi = (3.7 \pm 2.9)\mu K^2$ . This is negligible with respect to the CMB signal measured by the same experiment  $\ell(\ell+1)c_\ell/2\pi = (4700 \pm 540)\mu K^2$ . For the uncorrelated dust signal we set an upper limit to the contribution to the CMB power at 150GHz and  $\ell \sim 200$  of  $\ell(\ell+1)c_\ell/2\pi < 3\mu K^2$  at 95% C.L. .

*Subject headings:* interstellar matter, cosmology, cosmic microwave background

## 1. Introduction

The patchy emission of our Galaxy is a major concern for experiments designed to measure the anisotropy of the Cosmic Microwave Background (CMB). A "precision" phase, where temperature fluctuations are measured with a sensitivity of the order of tens of  $\mu K$  per pixel, has now begun (de Bernardis et al. 2000; Hanany et al. 2000). Forthcoming full-sky coverage space missions (MAP 2000; Planck 2000), and a host of future sub-orbital experiments are expected to reach sensitivities of a few  $\mu K$  per pixel . To fully exploit the potential of these new surveys, our knowledge of the diffuse emission of our Galaxy at high Galactic latitudes must improve as well.

At frequencies above  $\sim 100$  GHz this emission is dominated by thermal radiation from

large dust grains, heated by the interstellar radiation field to  $T_d \sim 10 - 30K$ . The ISD is distributed in filamentary "cirrus"-like clouds and covers the sky even at high Galactic latitudes (Low et al. 1984). The spectrum of this component in the 300 - 3000 GHz range has been mapped with coarse ( $7^\circ$ ) angular resolution and high sensitivity by the COBE-FIRAS experiment (Wright et al. 1991). The COBE-DIRBE maps provide higher angular resolution  $\sim 0.7^\circ$ , at  $> 1250$  GHz (Hauser et al. 1998; Arendt et al. 1998). Arcminutes resolution maps from the IRAS satellite are available only at  $> 3000$  GHz. These have been recalibrated using the COBE-DIRBE maps at 3000 and 1250 GHz (Schlegel et al. 1999), and extrapolated to longer wavelengths using a variety of physical models (Lagache et al. 1998; Finkbeiner et al. 1999; Lagache et al. 2000; Tegmark et al. 2000). At those longer wavelengths very few experimental data are available at subdegree resolution (see e.g. Masi et al. 1995; Masi et al. 1996; Lim et al. 1996; Leitch et al. 1997; de Oliveira-Costa 1997; Cheng et al 1997). "Anomalous" emission, morphologically correlated with the IRAS map but much larger than a naive extrapolation of thermal dust emission, has been detected in the microwaves (Kogut et al. 1996a; Kogut et al. 1996b; Lim et al. 1996; Leitch et al. 1997; de Oliveira-Costa 1997; de Oliveira-Costa et al. 1998; Mukherjee et al. 1999; Draine and Lazarian 1998; de Oliveira-Costa et al. 2000).

Here we analyze 90, 150, 240 and 410 GHz maps of 3% of the sky at Galactic latitudes  $10^\circ \lesssim b \lesssim 60^\circ$ . We compute the frequency and angular power spectrum of the fluctuations in these maps. We find that these maps are correlated with the emission mapped by IRAS extrapolated to our wavelengths using (Finkbeiner et al. 1999) model number 8. We will refer to this as FDS8 in the following. We also set upper limits to the level of residual, non-CMB structures, that are not correlated with FDS8.

## 2. Observations

We use the maps obtained from the 1998 long duration flight of the BOOMERanG experiment (de Bernardis et al. 2000), all pixelized with  $7'$  pixels and smoothed to a resolution of 22.5 arcmin FWHM. The instrument was calibrated against the CMB dipole at 90, 150, 240 GHz (10% uncertainty), and against the rms CMB anisotropy at 410GHz (20% uncertainty) (Crill et al. 2000). The conversion factors from CMB temperature fluctuations to brightness in our 4 bands are  $195, 426, 471, 204(MJy/sr)/K_{CMB}$  at 90, 150, 240 and 410 GHz respectively. We used a single channel at 90 and at 410 GHz, and combined 3 channels at 150 GHz and 3 channels at 240 GHz. About 1300 square degrees were observed at high galactic latitudes ( $-60^\circ \lesssim b \lesssim -20^\circ$ ;  $230^\circ \lesssim \ell \lesssim 270^\circ$ ; constellations of Caelum, Doradus, Pictor, Columba, Puppis), including a region with the lowest amount of dust emission of the full sky. In the observed region the fluctuation of the  $100 \mu\text{m}$  brightness mapped by IRAS is well below 1 MJy/sr in over 500 square degrees. The BOOMERanG maps have been obtained from the raw data using an iterative algorithm (Prunet et al. 2000). This reduces the large scale artifacts due to  $1/f$  noise, and correctly estimates the noise in the datastream, while producing a maximum likelihood map. Structures at scales larger than  $10^\circ$  are effectively removed in the process. This fact must be taken into account when comparing the BOOMERanG maps to other maps of the sky. In addition to the four frequencies mapped by BOOMERanG, we use the FDS8 dust maps as explained in next section.

## 3. The 410 GHz "dust monitor"

The highest frequency channel of the BOOMERanG photometer is centered at 410 GHz, with a FWHM of 26 GHz. At this frequency, the brightness of the CMB is smaller than at our lower frequencies, while thermal emission from Galactic dust is much larger.

The 410 GHz map of the sky obtained by BOOMERanG is dominated by faint cirrus clouds at intermediate Galactic latitudes ( $-10^\circ < b < -20^\circ$ ). In fig.1 we compare our 410 GHz map (top panel) to the FDS8 extrapolation of the IRAS map (middle panel) obtained as follows. FDS8 assumes two components of ISD with different temperature and spectral index of dust emissivity. The two temperatures depend on the observed direction. On the average  $\langle T_{d,1} \rangle \sim 16.2K$ ,  $\langle T_{d,2} \rangle \sim 9.4K$ , and the average ratio between dust brightness at 3000 GHz and dust brightness at 410 GHz is  $\sim 13$ . The extrapolated map has been sampled along the scans of the 410 GHz channel of BOOMERanG, and then high-pass and low-pass filtered using the 410 GHz detector transfer function, in order to create a synthesized time-stream. The time stream has been processed in the same way as the BOOMERanG data, and smoothed to 22.5 arcmin to obtain the map shown in the middle panel of fig.1. The morphological and amplitude agreement of the two maps provides evidence that the 410 GHz data represent a good monitor for interstellar dust emission in the BOOMERanG data. Bright compact structures apparent in the difference map (lower panel in fig.1) correspond to the dense, cool cores of clouds that are not well modelled in FDS8. The remaining structures are mostly due to residual noise in the BOOMERanG data. In a similar way we obtained extrapolated maps for the other BOOMERanG channels.

We have computed the power spectrum of the 410 GHz map in three circular regions, each  $18^\circ$  in diameter, centered at  $(RA, dec, b) = (107^\circ, -47^\circ, -17^\circ)$ ,  $(92^\circ, -48^\circ, -27^\circ)$ ,  $(74^\circ, -46^\circ, -38^\circ)$  i.e. low, intermediate and high Galactic latitudes respectively. We used a spherical harmonics transform and corrected for the finite size of the cap, for filtering applied in the time domain, and for the contribution of instrumental noise (Hivon et al. 2001). The results are shown in figure 2. The contribution of CMB anisotropy to these spectra is computed to be negligible. The errors have been computed by adding two contributions. The first one is an estimate of instrumental noise. The second is an estimate of sampling variance (see e.g. Scott et al. 93) for a gaussian field having the same power spectrum. The

latter has to be included if we want to consider the measured spectrum as representative of ISD fluctuations in the Galaxy in general. The spectrum at the highest Galactic latitude is basically an upper limit for dust fluctuations, since the residual fluctuations are comparable to our estimate of detector noise plus CMB anisotropy. The spectra at low and intermediate latitudes are well fit by a power law  $c_l \sim \ell^{-\beta}$  as in previous studies based on IRAS and DIRBE maps (Gautier et al. 1992; Low and Cutri 1994; Guarini et al. 1995; Wright 1998; Schlegel et al. 1999). We find a power law exponent  $2 \lesssim \beta \lesssim 3$ , consistent with the studies cited above, thus extending this result to wavelengths very close to those used for CMB studies. The power spectra of FDS8 at 410 GHz in the same regions are also shown in fig.2 for comparison. The agreement is very good for the region centered at  $b = -17^\circ$ , where detector noise is negligible. The agreement is also good in the region centered at  $b = -27^\circ$ , but a systematic amplitude difference is evident. We estimate upper limits for the fluctuations due to any dust component not correlated with IRAS by computing the spectrum of the difference map obtained removing the F8 map from the measured 400GHz map. The upper limits are of the same order of magnitude of the errors in the measured power spectrum of the 400 GHz map.

#### 4. Pixel-pixel correlations

We made pixel-pixel correlations between our four maps and the corresponding FDS8 maps. The signal in each of our channels is a linear combination of Galactic emission, CMB anisotropies and noise. The relative weight of the Galactic and the CMB components depends on the Galactic latitude and on the frequency of the channel. The advantage of correlating with the FDS8 maps is that the noises are uncorrelated, and at 3000 GHz the CMB is totally negligible. Any detected correlation is thus due to Galactic emission. In the BOOMERanG 410 GHz channel we expect to have little CMB anisotropy and dominant

Galactic dust emission, at least at  $b > -20^\circ$ . In fact, in this latitude range the pixel-pixel scatter plot of our 410 GHz channel vs FDS8 at 410 GHz has a best fit line with slope  $(0.644 \pm 0.038)$ , a highly significant correlation. This result has been obtained using a jack-knife technique: we divide the latitude band  $-20^\circ < b < -10^\circ$  into five  $10^\circ \times 10^\circ$  regions and we compute the best fit slope for each of the regions. We then compute the average and standard error on the average as our best estimate of the general slope. In this way we properly take into account the fact that deviations from an ideal correlation are dominated by fluctuations in dust properties, rather than by detector noise. The slopes and Pearson’s linear correlation coefficients are listed in table 1. As we move towards lower frequencies, the correlation at a given latitude range gets worse, but is still significant. We have converted the measured slopes into brightness ratios  $R_i = \Delta B_i / \Delta B_{IRAS}$  using the spectral response of the BOOMERanG bands. The spectrum of the brightness ratios is plotted in fig.3 (triangles). We compare it to an empirical model assuming a power law  $B(\nu) \sim \nu^\alpha$ . We find a best fit  $\alpha = (3.2 \pm 0.3)$  at  $b > -20^\circ$ . In FDS8 model,  $\alpha = 3.15$  in the range 240-410GHz, while  $\alpha = 3.36$  in the range 240-150GHz.

At higher Galactic latitudes (four  $10^\circ$  wide latitude bands at  $b < -20^\circ$ ) we find poorer but still significant correlations at 410 GHz and 240 GHz, while the correlation is just marginal at 150 GHz, and is negligible at 90 GHz (see table 1 and squares in fig.3). Here we get a best fit  $\alpha = (4.3 \pm 1.0)$ .

## 5. Contamination of CMB measurements at high Galactic latitudes

We can use the measured ratios  $R_i$  to estimate the rms fluctuation due to IRAS-correlated emission at high Galactic latitudes. We have simply  $var(\Delta B_i) = R_i^2 var(\Delta B_{IRAS})$ . We divide the observed region in latitude ranges,  $10^\circ$  wide, and list the computed mean square fluctuations in table 2. The mean square fluctuation is dominated by signals at the

lowest multipoles, due to the falling power spectrum of dust  $c_\ell \sim \ell^{-2.5}$ . So at multipoles corresponding to the first acoustic peak of the CMB anisotropy the dust contamination is even more negligible with respect to the CMB fluctuations. We compute the power spectrum in band  $i$  with the simple scaling formula  $c_{\ell,i} = \frac{R_i^2}{R_{410}^2} c_{\ell,410}$  where  $R_i$  is the average ratio between the dust signal in band  $i$  and the IRAS/DIRBE signal. The result is plotted in fig.4 for the extrapolation of the 410 GHz spectrum centered at  $b = -27^\circ$ . Due to the poor correlation, only upper limits are found for the 90 GHz band (at a level similar to the power spectrum estimates for the 150 GHz channel), which are not plotted. It is evident that at  $\ell > 100$  the dust signals at 90 and 150 GHz are negligible with respect to the cosmological signal. These estimates of contamination are consistent with the dust foreground model of (Tegmark et al. 2000) (compare their fig.3 with our fig.4). If we scale to 150 GHz the upper limits for the uncorrelated component, assuming the same spectral ratios, we get 95% C.L. upper limits  $\ell(\ell + 1)c_\ell/2\pi \lesssim 5\mu K^2$  at 95% C.L. for  $50 \lesssim \ell \lesssim 600$ .

## 6. Conclusions

BOOMERanG has detected thermal emission from interstellar cirrus at intermediate and high Galactic latitudes. The 410 GHz map is morphologically very similar to extrapolation of the IRAS(3000GHz) and DIRBE(1250GHz) maps. The angular power spectrum of the dust dominated 410 GHz map is a power law  $c_\ell \sim \ell^{-\beta}$  with  $2 \lesssim \beta \lesssim 3$ . We have detected a component correlated with the IRAS/DIRBE map in all the BOOMERanG bands at  $-10^\circ > b > -20^\circ$ , and in the 150, 240 and 410 GHz bands at higher Galactic latitudes. This dust contamination is negligible with respect to the CMB anisotropy at high Galactic latitudes, accounting for less than 1% of the total angular power spectrum for multipoles  $\ell > 100$  at  $\nu < 180GHz$ .



The BOOMERanG program has been supported by NASA and NSF in the USA, by ASI, PNRA, University La Sapienza in Italy, by PPARC in UK and by NSERC and University of Toronto in Canada.

## REFERENCES

- de Bernardis et al. 2000, *Nature*, 404, 955-959
- Hanany et al. 2000, submitted to *Ap.J.*, astro-ph/0005123
- <http://map.gsfc.nasa.gov>
- <http://astro.estec.esa.nl/Planck>
- Low F.J. et al. 1984, *Ap.J.* 278, L19.
- Wright E.L. et al. 1991, *Ap.J.* 381, 200.
- Schlegel D.J. et al. 1999, *Ap.J.* 500, 525.
- Finkbeiner D.P. et al. 1999, *Ap.J.*, 524, 867.
- Masi S. et al. 1995, *Ap.J.*, 452, 253.
- Masi S. et al. 1996, *Ap.J.*, L47, 463.
- Lim et al. 1996, *Ap.J.*, 469, L69.
- Leitch E., et al. 1997, *Ap.J.*, 486, L23.
- de Oliveira-Costa 1997, *Ap.J.*, 482, L17.
- Cheng E., et al., 1997, *Ap.J.*, 488, L59.
- Lagache G. et al., 2000, *Astron. Astrophys.* 344, 322.
- Lagache G. et al., 1998, *Astron. Astrophys.* 333, 709.
- de Oliveira-Costa 1998, *Ap.J.*, 509, L9.
- Mukherjee et al. 1999, submitted to *MNRAS*, astro-ph/0002305

Hauser M.G. et al., 1998, Ap.J., 508, 25.

Arendt R.G. et al., 1998, Ap.J., 508, 74.

Kogut A. et al., 1996a, Ap.J., 460, 1.

Kogut A. et al., 1996b, Ap.J., 464, L5.

Draine B.T., and Lazarian A., 1998, Ap.J., 508, 157.

de Oliveira-Costa et al. 2000, astro-ph/0010527

Crill B. et al., 2000, in preparation

Prunet S. et al., 2000, in "Energy densities in the Universe", XXth Rencontre de Moriond,  
Bartlett J., Dumarchez J. eds., Editions Frontieres, Paris - astro-ph/0006052

Scott, D., Srednicki, M., White, M. 1993, ApJ, 421, L5

Hivon et al. in preparation

Gorski K.M., Hivon E. and Wandelt B.D., "Analysis Issues for Large CMB Data Sets",  
1998, Proceedings of the MPA/ESO Conference, Garching 2-7 August 1998,  
eds. A.J. Banday, R.K. Sheth and L. Da Costa, (astro-ph /9812350); see also  
<http://www.tac.dk/healpix/>

Gautier T.N. III, et al., 1992, A.J., 103, 4.

Low F.J. and Cutri R.M., 1994, Infrared Phys. Techn., 35, 291.

Guarini G. et al., 1995, Ap.J. 442, 23.

Wright E.L., 1998, Ap.J. 496, 1.

Tegmark M. et al., 2000, Ap.J. 530, 133.



Fig. 1.— PLATE Top panel: BOOMERanG map at 410GHz. The map has been obtained by coadding the data in  $7'$  healpix pixels (Gorski et al. 1998) and applying a gaussian smoothing to an equivalent resolution of 22.5 arcmin. At this frequency  $1mK_{CMB} = 0.20$  MJy/sr. Due to the map-making technique, structures with angular scales larger than  $10^\circ$  have been effectively removed from the map. Middle panel: FDS8 extrapolation at 410 GHz of the IRAS map, in the same sky region. This map has been high and low-pass filtered as in the BOOMERanG 410 GHz channel (see text) for a meaningful comparison. Bottom panel: residuals after subtraction of the FDS8 map from the BOOMERanG 410 GHz map. The three circles identify the regions where we carried out the power spectrum analysis.

Fig. 2.— Angular power spectrum of the BOOMERanG 410 GHz map, for three disks with diameter  $18^\circ$ , centered at different Galactic latitudes (squares,  $b = -17^\circ$ ; circles,  $b = -27^\circ$ ; down triangles,  $b = -38^\circ$ ). At the highest latitude the signal is small with respect to the detector noise, and we consider the spectrum as an upper limit for dust brightness fluctuations. Best fit power-law spectra  $c_l \sim \ell^{-\beta}$  are shown as continuous lines and labelled by their best fit slope  $\beta$ . The dashed lines are the power spectrum of the FDS8 map at 410 GHz in the same sky regions. The large thin error bars include cosmic/sampling variance, while the smaller thick ones are from intrumental noise only.

Fig. 3.— Ratio between the dust brightness fluctuations in the BOOMERanG bands and the dust brightness fluctuations detected by IRAS/DIRBE. Triangles indicate measurements at intermediate Galactic latitudes ( $-20^\circ < b < -10^\circ$ ), while circles indicate measurements at high Galactic latitudes ( $b < -20^\circ$ ). The best fits assuming a power law spectrum with spectral index  $\alpha$  are plotted as lines, and are labelled by the best fit value for  $\alpha$ . The dashed line is the average FDS8 spectrum, normalized to the BOOMERanG measurement at 410 GHz at intermediate latitudes.

Fig. 4.— Angular power spectra of dust emission in a disk centered at RA=92°, dec=-48°, b=-

$27^\circ$  that is correlated with the FDS8 IRAS extrapolation, at 150GHz (filled down triangles) and at 240GHz (filled up triangles). The power spectrum of the microwave sky at 150 GHz (de Bernardis et al. 2000) is shown for comparison as filled circles. For the dust spectra the error bars include the uncertainty due to the partial correlation between our data and the FDS8 extrapolated IRAS data. The 90 GHz correlation is so poor that we only find upper limits (not plotted here) similar to the 150 GHz values. It is evident that in this region of the sky the Galactic dust signal is negligible with respect to the CMB signal at these frequencies.

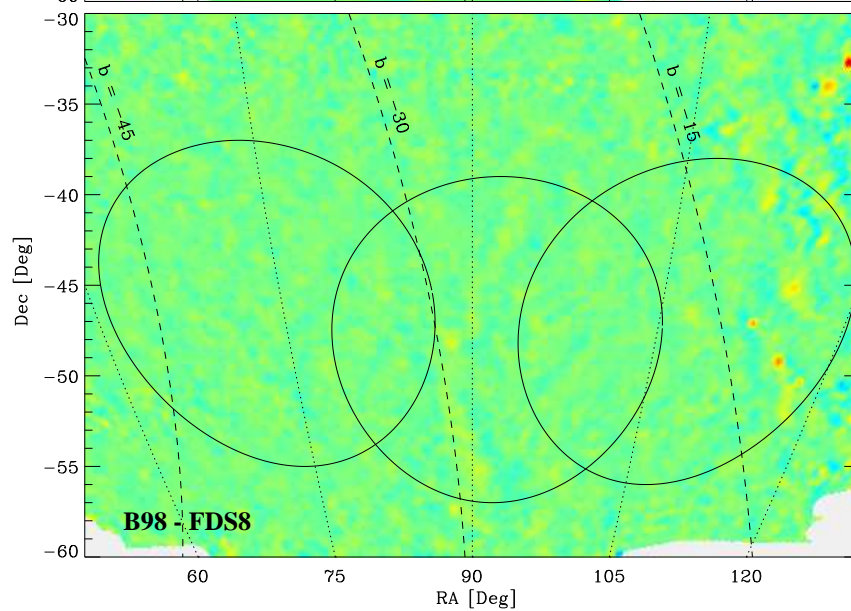
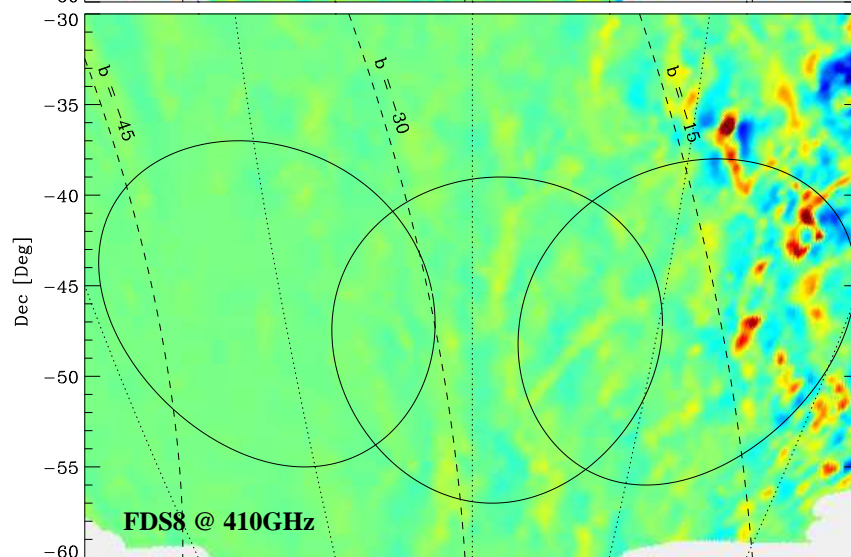
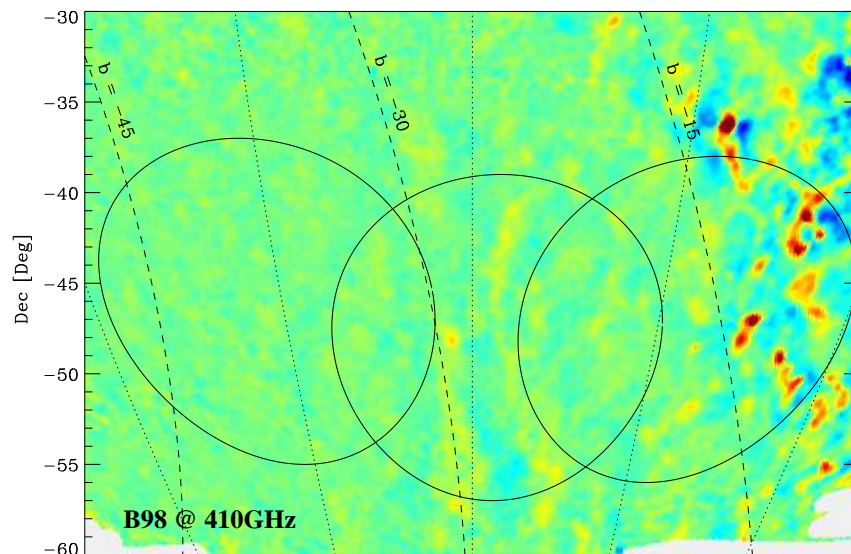
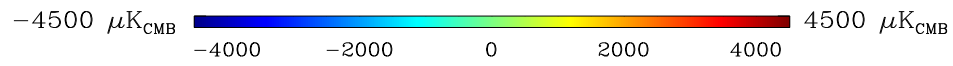
Table 1. Correlation between BOOMERanG data and IRAS/DIRBE data extrapolated to 410 GHz (FDS8).

Band Center (GHz)	slope $R$ [ $\mu K_{CMB}/(MJy/sr)$ ] (Pearson's $R$ )	
	$-20^\circ < b < -10^\circ$ (22843 pixel)	$b < -20^\circ$ (68987 pixel)
410	$(3200 \pm 190)$ (0.298)	$(4700 \pm 1500)$ (0.138)
240	$(254 \pm 46)$ (0.156)	$(258 \pm 52)$ (0.041)
150	$(93 \pm 23)$ (0.085)	$(46 \pm 29)$ (0.003)
90	$(58 \pm 49)$ (0.032)	$(-20 \pm 110)$ (-0.028)

Table 2. Estimated rms fluctuations due to dust emission  $\langle \Delta T_{dust}^2 \rangle^{1/2}$  ( $\mu K_{CMB}$ )  
(angular scales between 22 arcmin and  $10^\circ$ ).

Band Center (GHz)	$-20^\circ < b < -10^\circ$	$-30^\circ < b < -20^\circ$	$-40^\circ < b < -30^\circ$	$-50^\circ < b < -40^\circ$	$-60^\circ < b < -50^\circ$
410	$(680 \pm 40)$	$(280 \pm 90)$	$(180 \pm 60)$	$(110 \pm 35)$	$(120 \pm 40)$
240	$(54 \pm 10)$	$(15 \pm 3)$	$(9.6 \pm 2.0)$	$(6.0 \pm 1.2)$	$(6.4 \pm 1.3)$
150	$(20 \pm 5)$	$(2.8 \pm 1.7)$	$(1.7 \pm 1.1)$	$(1.1 \pm 0.7)$	$(1.2 \pm 0.7)$
90	$(12 \pm 10)$	$< 12 (2\sigma)$	$< 7 (2\sigma)$	$< 5 (2\sigma)$	$< 5 (2\sigma)$





RA [Deg]

